**Molecular Cell, Volume *81***

## Supplemental information

# Stress-induced nuclear condensation of NELF drives transcriptional downregulation

**Prashant Rawat, Marc Boehning, Barbara Hummel, Fernando Aprile-Garcia, Anwit S. Pandit, Nathalie Eisenhardt, Ashkan Khavaran, Einari Niskanen, Seychelle M. Vos, Jorma J. Palvimo, Andrea Pichler, Patrick Cramer, and Ritwick Sawarkar**

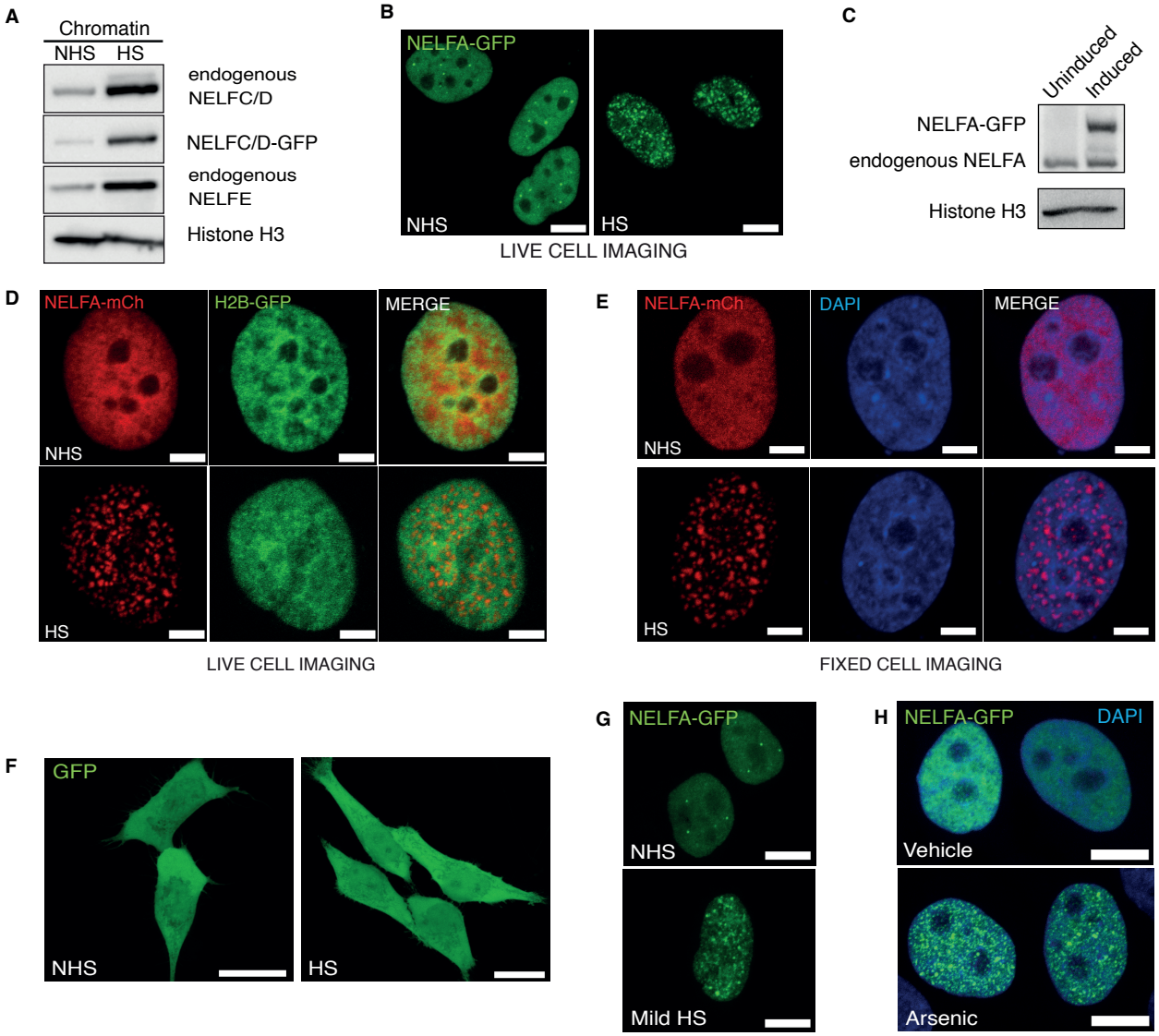


Figure S1 - NELF condensation in nuclei upon stress, Related to Figure 1

**Figure S1. NELF condensation in nuclei upon stress, Related to Figure 1.**

A. Western blot analysis of indicated proteins in isolated chromatin fractions from HeLa cells exposed to heat shock (HS) compared to non-heat-shocked cells (NHS). Histone H3 serves as normalization control.
B. Fluorescence microscopy images of live HeLa cells expressing NELFA-GFP. NHS: No heat shock; HS: heat shock. Scale bar indicates 10 μm.
C. Western blot analysis of NELFA in HeLa cell extracts expressing Tetracycline inducible NELFA-GFP. Cells were either not induced or induced with 1 μM tetracycline (Methods).
D. Fluorescence microscopy images of HeLa cells showing NELFA-GFP, histone H2B and merged signal in living cells. NHS: No heat shock; HS: heat shock. Scale bar indicates 5 μm.
E. Fluorescence microscopy images of HeLa cells expressing NELFA-mCherry. NHS: No heat shock; HS: heat shock. Scale bar indicates 5 μm.
F. Fluorescence microscopy images of live (unfixed) HeLa cells expressing GFP. NHS: No heat shock; HS: heat shock. Scale bar indicates 5 μm.
G. Fluorescence microscopy images of HeLa cells exposed to mild HS (at 42°C) or control conditions (NHS) showing NELFA-GFP signal. Scale bar indicates 10 μm.
H. Fluorescence microscopy images of HeLa cells exposed to arsenic or vehicle showing merged NELFA-GFP and DAPI images. Scale bar indicates 10 μm.

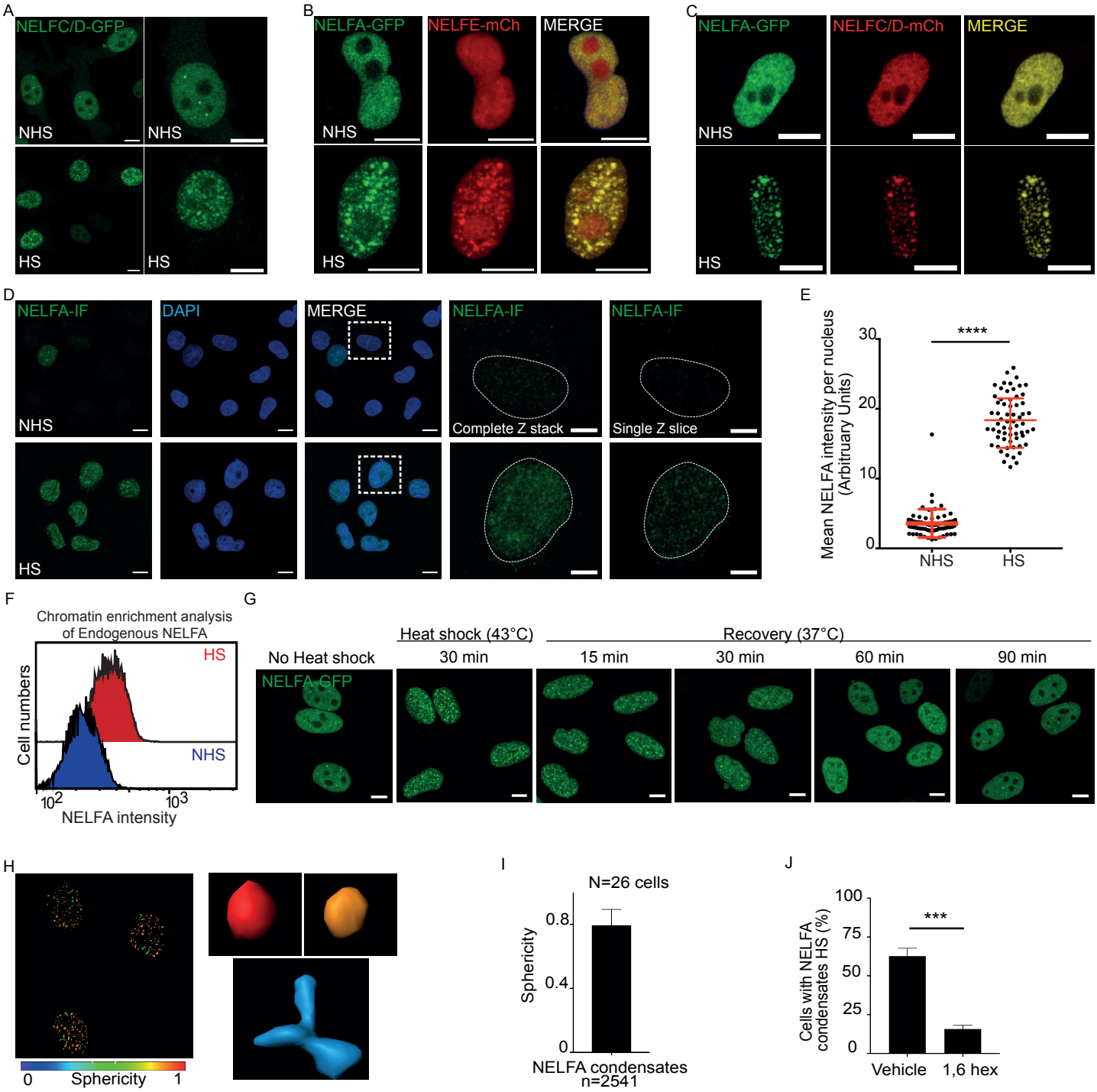


Figure S2 - Characterization of NELF condensates formed upon heat shock, Related to Figure 1

**Figure S2. Characterization of NELF condensates formed upon heat shock, Related to Figure 1.**

A. Fluorescence microscopy images of HeLa cells expressing NELFC/D-GFP. Enlarged images on the right. NHS: No heat shock; HS: heat shock. Scale bar indicates 10 μm.
B. Co-localization of transfected NELFE-mCherry and NELFA-GFP protein in HeLa cells. NHS: No heat shock; HS: heat shock. Scale bar indicates 10 μm.
C. Co-localization of transfected NELFC/D-mCherry with NELFA-GFP protein in HeLa cells. NHS: No heat shock; HS: heat shock. Scale bar indicates 10 μm.
D. Immunofluorescence images of HeLa cells showing chromatin-associated endogenous NELFA (green), DAPI and merged signal. Scale bar indicates 10 μm. Cells demarcated in merge panel are shown at higher magnification as complete z stack of images or as a single z slice image (Scale bar indicates 5 μm).
E. Data quantification of experiment described in D. Asterisks denote P-value of <0.0001 as calculated by two-tailed unpaired t-test.
F. FACS analysis of chromatin-associated endogenous NELFA stained with a NELFA antibody in wild-type HeLa cells. Non chromatin- associated proteins were pre-extracted prior to FACS analysis (see methods). NHS: No heat shock; HS: heat shock.
G. Fluorescence microscopy images of HeLa cells exposed to heat shock (HS) or recovery following HS for indicated time points showing NELFA-GFP. Scale bar indicates 10 μm.
H. Sphericity analysis of NELFA-GFP condensates shown in cells exposed to heat shock. The sphericity is calculated using Imaris 9.1 software and represented as the
sphericity index on the color scale of 0 (non-spherical) to 1 (perfect spheres). The boxes on the right show individual exemplary NELF condensates.
I. The histogram represents quantification of sphericity indices of 2541 condensates of NELFA from 26 cells.
J. Percentage of cells with NELFA condensates after heat shock in vehicle- or 1,6 hexanediol (1,6 hex)-treated HeLa cells expressing NELFA-GFP. Data quantification of Fig 1F. Error bars represent S.D. (n = 2, biologically independent replicates). Number of cells (N) = 185 and 176 respectively. Asterisks denote P-value of 0.001 ascalculated by two-tailed unpaired t-test.

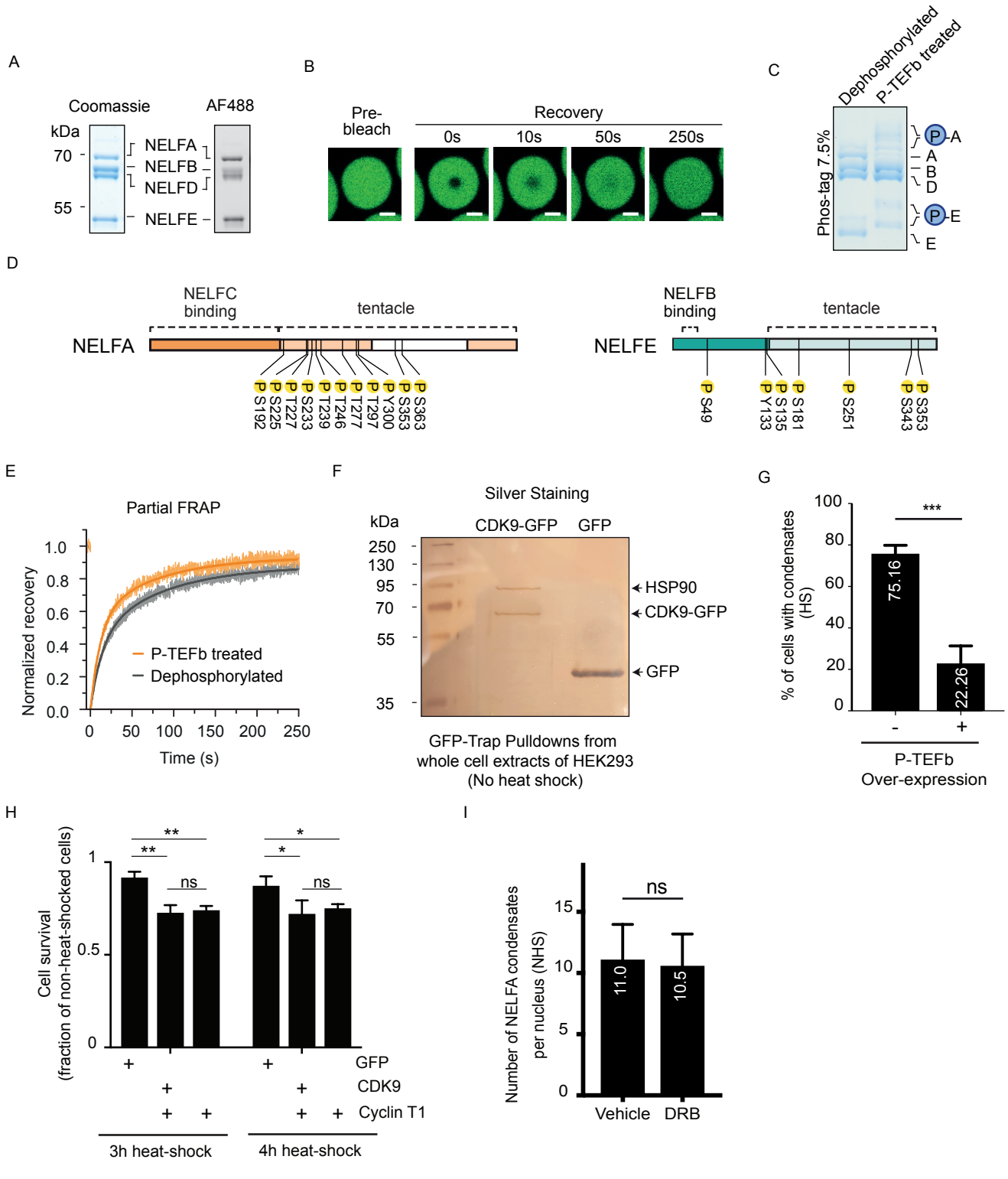


Figure S3 - Consequences of CDK9 mediated NELF phosphorylation *in vitro* and *in vivo*
Related to Figure 2, 3 and 4

**Figure S3. Consequences of CDK9 mediated NELF phosphorylation in vitro and in vivo. Related to Figure 2, 3 and 4.**

A. Coomassie-stained SDS-PAGE analysis of purified recombinant NELF complex composed of NELFA, NELFB, NELFD and NELFE. SDS–PAGE fluorescence scan of NELF complex after chemical labeling using an amine-reactive Alexa Fluor 488 (AF488) dye.
B. Microscopy images of the fluorescence recovery after partial photobleaching a NELF droplet. Exemplary images from the experiment in Figure 2D are shown. Recovery time is indicated in seconds (s). Scale bar indicates 2 µm.
C. Phosphate-affinity (Phos tag) SDS-PAGE analysis of dephosphorylated and P-TEFb treated NELF complex (Methods). P-TEFb phosphorylates only NELFA and NELFE subunits of the NELF complex.
D. Mass spectrometry-based analysis of recombinant NELF complex incubated with PTEFb in vitro. The position of 18 residues of NELFA and NELFE found to be phosphorylated are indicated, in line with (Vos et al., 2018a).
E. Relative fluorescence recovery kinetics of dephosphorylated (grey) and P-TEFb treated (orange) NELF following partial droplet bleaching.. The curve shows the mean and standard error (light grey or orange) across five FRAP experiments and was fit to a double-exponential recovery curve (dark grey or orange).
F. Silver-stained SDS-PAGE of immunoprecipitates using GFP-Trap from HEK293 cells expressing CDK9-GFP and GFP proteins. CDK9-GFP pulls down nearly equimolar levels of molecular chaperone HSP90 as confirmed by mass spectrometry.
G. Percentage of cells with NELFA condensates after heat shock as measured using NELFA-mCherry. P-TEFb over-expression was carried out by expressing CDK9-GFP and CCNT1-GFP vectors together. Error bars represent S.D. (n = 3, independent cell culture replicates). Asterisks denote P-value 0.001 as calculated by two-tailed unpaired t-test.
H. Fraction of living HeLa cells after exposure to heat shock (HS) for the indicated time and subsequent recovery for 24 hours. The data were normalized to the number of living HeLa cells under respective no heat shock (NHS) conditions. Indicated proteins were ectopically expressed in HeLa cells. Error bars represent S.D. (n= 3, independent cell culture replicates). Asterisks denote P-value (**: 0.01; *: 0.05) as calculated by 2-way ANOVA for multiple comparisons (Sidak's multiple comparison test). ns denotes non-significant.
I. Graph showing number of NELFA condensates under no heat shock in HeLa cells treated with vehicle or DRB for 60 minutes. ns denotes non-significant as calculated by two-tailed unpaired t-test.

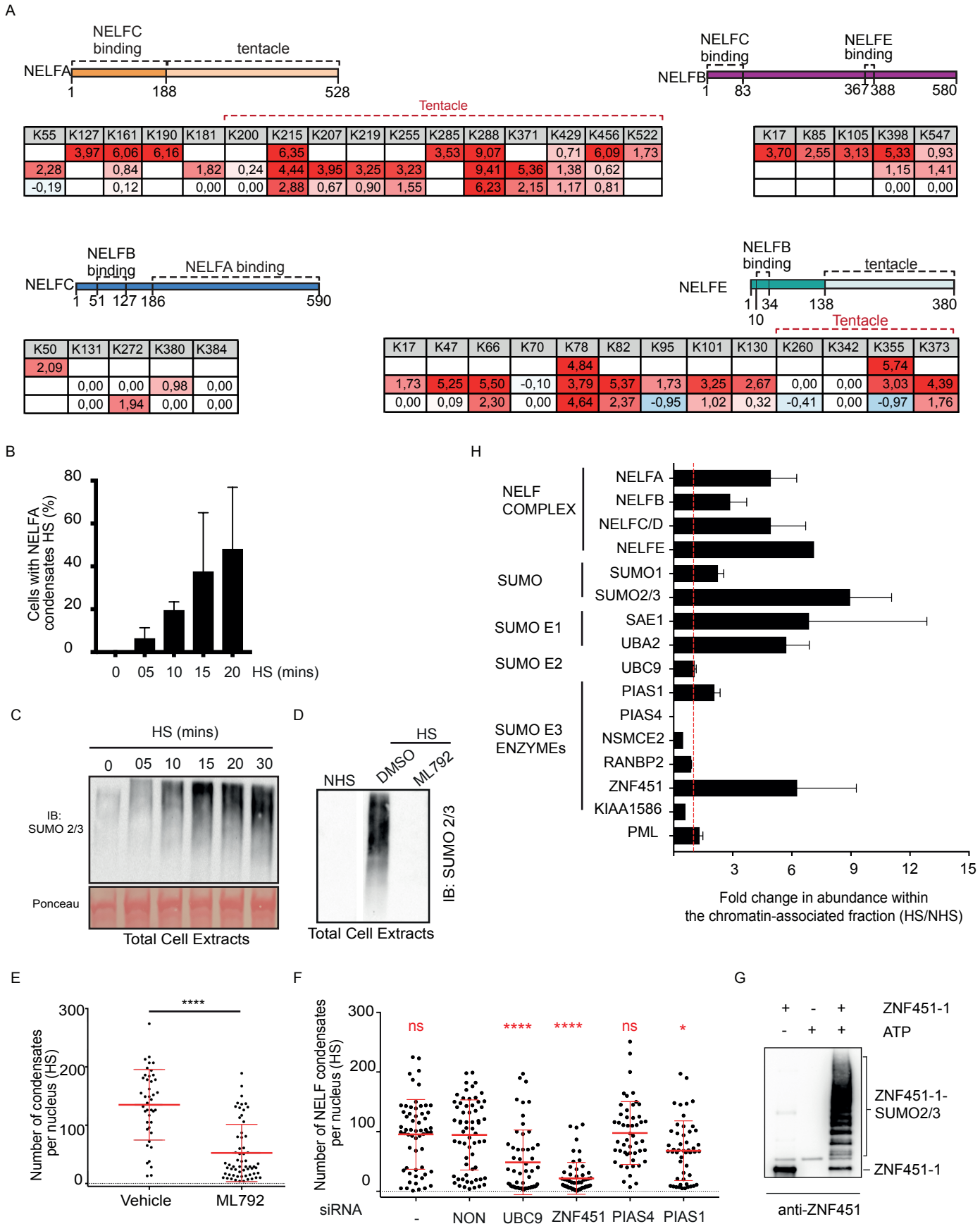


Figure S4 - Stress-induced SUMOylation is required for NELF condensation
Related to Figure 4

**Figure S4. Stress-induced SUMOylation is required for NELF condensation, Related to Figure 4.**

A. Mass spectrometry-based analyses of SUMOylation of NELF complex members. Different complex members of NELF are shown, each with a scheme showing amino-acid positions delimiting different domains (top) along with log2 fold-change in SUMOylation upon HS (bottom table). The amino-acid positions are taken from NELFA (protein ID: A0A0C4DFX9), NELFB (protein ID: Q8WX92), NELFC (protein ID: Q8IXH7), NELFE(protein ID: P18615). The data are taken from (Hendriks et al., 2018; Hendriks et al., 2017) and are from different cell lines - top row: HEK293, middle row: HeLa, bottom row: U2OS.
B. Graph showing percentage of HeLa cells with NELFA condensates with increasing duration of heat shock. Error bars represent S.D. (n = 2, independent replicates).
C. Western blot analysis of SUMO2/3 protein in HeLa cells exposed to heat shock (HS) for different time durations.
D. Western blot analysis of SUMO2/3 protein in HeLa cells exposed to no heat shock (NHS), or heat shock (HS) and treated with either vehicle or ML-792. The lanes between NHS and HS are removed from the blot. Indicated with white line gap within the represented blot.
E. Graph showing the number of NELFA-GFP condensates per nucleus in HeLa cells exposed to indicated conditions. Each dot represents data for one nucleus. Asterisks denote P -value of <0.0001 as calculated by two-tailed unpaired t-test.
F. Graph showing the number of NELFA-GFP condensates per nucleus in HeLa cells exposed to indicated conditions. Quantification for Figure 4E. Each dot represents data for one nucleus. Asterisks denote P -value of (****: <0.0001; *: 0.05) as calculated by one-way ANOVA with Dunnett's multiple comparison tests. ns denotes non-significant P-values. All P-values shown are calculated in comparison with siNON.
G. Western blot after in vitro SUMOylation reaction using the ZNF451 antibody. The reaction contained purified recombinant NELF complex with SUMO E1 activating enzyme, SUMO E2 conjugating enzyme, SUMO2/3 and the purified recombinant catalytic N-terminal of ZNF451 isoform 1. Reactions lacking ATP or E3 ligase ZNF451 are used as negative controls.
H. Mean fold changes in abundance of chromatin-associated NELF complex, SUMO machinery and SUMO proteins and PML upon heat shock detected by SILAC based Mass Spectrometry. The chromatin fractions were prepared from HEK293 cells in no heat shock (HS) or heat shock (HS) conditions. Error bars represent S.D. (n = 3 independent cell cultures).

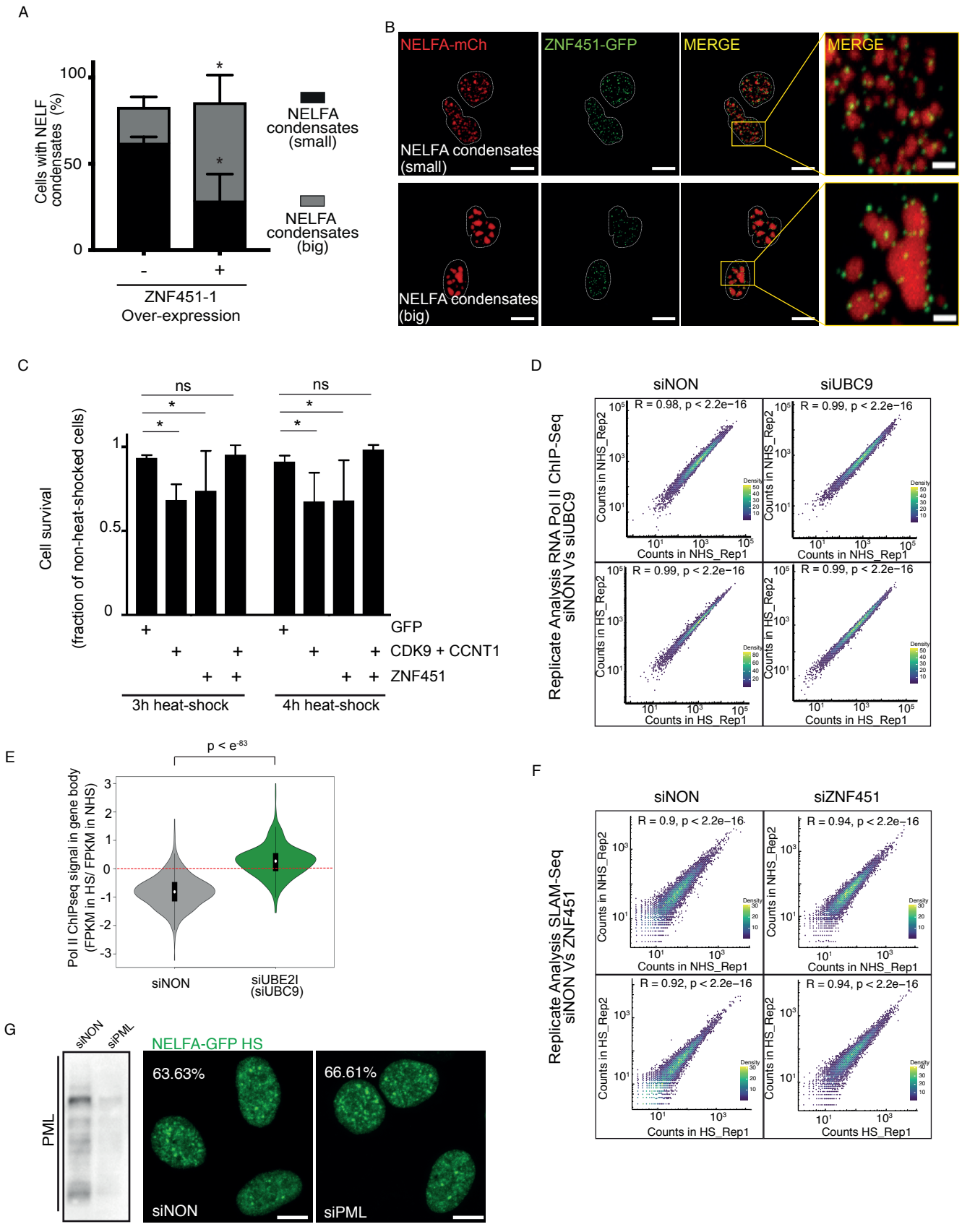


Figure S5 - ZNF451 promotes NELFA condensation in cells
Related to Figure 4

**Figure S5. ZNF451 promotes NELFA condensation in cells, Related to Figure 4.**

A. Graph showing the number of NELFA-GFP condensates per nucleus in HeLa cells exposed to heat shock in presence or absence of over-expression of ZNF451-1. The Condensates are divided in two indicated categories based on their sizes; Error bars indicate S.D. (n=3 independent cell cultures). Asterisks denote P-value 0.05 as calculated by two-tailed unpaired t-test.
B. Fluorescence microscopy images of HeLa cells expressing mCherry fused NELFA and GFP fused ZNF451 (Isoform 1) upon heat shock. Scale bar indicates 10 μm. Subset showing enlarged section of a single cell in merged channel image (scale bar indicates 2 μm).
C. Fraction of living HeLa cells after exposure to heat shock (HS) for the indicated time and subsequent recovery for 24 hours. The data were normalized to the number of living HeLa cells under respective no heat shock (NHS) conditions. Indicated proteins were ectopically expressed in HeLa cells. Error bars represent S.D. (n = 3 independent cell culture). Asterisks denote P-value 0.05 as calculated by 2-way ANOVA for multiple comparisons (Sidak's multiple comparison test). ns denotes non-significant.
D. Correlation of normalized counts in gene body regions (TSS +1.5 kb to TES – 0.5kb) from RNA-Pol II ChIP-Seq datasets (siNON and siUBC9) between replicates. R and p values are calculated using spearman correlation method.
E. Effect of SUMO E2 (UBC9) depletion on HS-induced changes in RNA pol II ChIP-seq occupancy in gene bodies of VCaP cells. Top 250 expressed genes in siNON NHS condition were used for the analysis. The violin plot depicts median, interquartile range and 95%-confidence interval with white dot, black bar and thin black line, respectively. P-value from Wilcoxon test is indicated.
F. Correlation of normalized counts in 3'UTR regions from SLAM-Seq datasets (siNON and siZNF451) between replicates. R and p values are calculated using spearman correlation method.
G. Left: Western blot analysis of PML protein in HeLa total extracts treated with siRNA non-targeting (siNON) or siRNA PML (siPML). Right, Fluorescence microscopy images of HeLa NELFA-GFP cells treated with siNON or siPML under heat shock condition (HS). % Values shown on the images indicate the fraction of cells with NELF condensates. Scale bar indicates 10 μm.

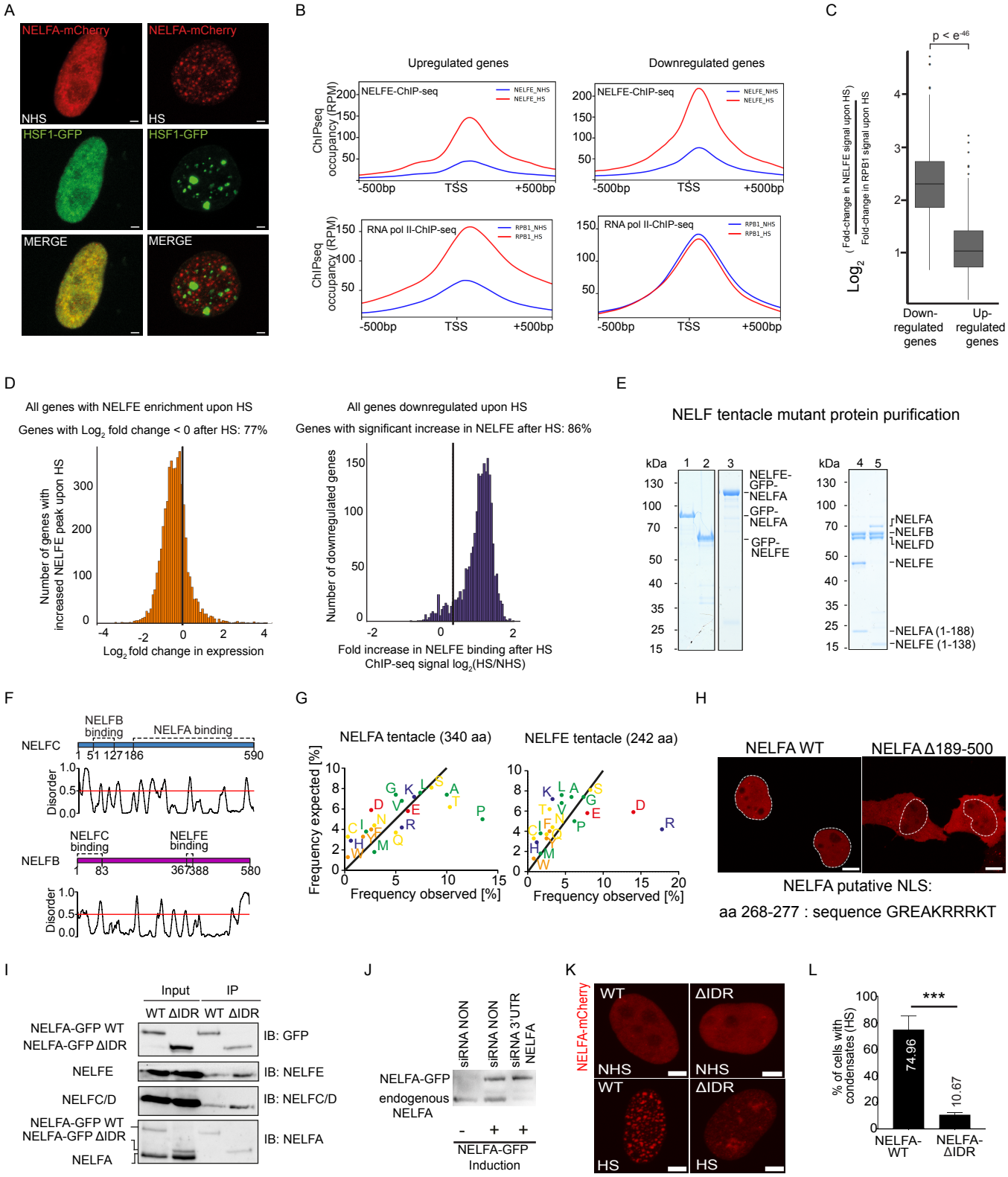


Figure S6 - Generation and characterization of NELF tentacle and IDR deletion mutants
Related to Figure 5 and 6

**Figure S6. Generation and characterization of NELF tentacle and IDR deletion mutants, Related to Figures 5 and 6.**

A. Fluorescence microscopy images of HeLa cells expressing mCherry fused NELFA and GFP fused HSF1. NHS: No heat shock; HS: heat shock. Scale bar indicates 10 μm.
B. Profile plots of NELFE and RNA Pol II binding around TSS (+/- 500 bp) for genes which are significantly upregulated or downregulated according to DESeq2 analysis in K562 cells (Aprile-Garcia et al., 2019).
C. Ratio of NELFE to Pol II occupancy at TSS of genes shown in panel B is depicted as box plot. Box plots display the 25th to 75th percentiles (boxes), medians (lines) and 1.5× the interquartile range (whiskers). Outliers are depicted as individual dots. Significance is calculated using Wilcoxon test.
D. Analysis of genes to establish a correlation between NELFE enrichment and downregulation upon heat-shock. (Left) Fold change in gene expression is shown as frequency histogram. All genes with significant increase in NELFE binding were used for this analysis. (Right) NELFE occupancy at promoters (TSS +/- 500bp) is shown as a frequency histogram. All genes which are significantly downregulated were used in this analysis.
E. Coomassie-stained SDS-PAGE of purified recombinant proteins. 1; GFP protein fused with NELFA tentacle region (residues 189-528). 2; GFP protein fused with NELFE tentacle region (residues 139-380). 3; double tentacle GFP protein with NELFE and NELFA tentacles fused to the C- and N-terminus respectively. 4; NELF complex variant lacking the NELFA tentacle (ΔNELFA tentacle). 5; NELF complex variant lacking the NELFE tentacle (ΔNELFE tentacle).
F. Domain architecture and disorder prediction of the NELFC and NELFB subunits. Intrinsically disordered regions are predicted using PONDR software. The definition of protein domains is taken from (Vos et al., 2018b).
G. Sequence analysis of both NELFA (residues 189-528) and NELFE (residues 139-380) tentacle regions. The relative amino acid abundance was plotted for each residue against the relative abundance within vertebrate proteins (King and Jukes, 1969). Amino acids are color-coded based on their physicochemical properties: Negatively charged, red; positively charged, blue; polar, yellow; aromatic, orange; aliphatic, green.
H. Fluorescence microscopy images of HeLa cells expressing mCherry fused to either wild-type NELFA (WT) or NELFA lacking the tentacle region (residue 189-500). Nucleus is marked with white dashed lines. Scale bar indicates 10 μm.
I. Immunoblot (IB) analysis of indicated NELF proteins in input and GFP-trap immunoprecipitates (IP) from HeLa cells. The cells stably expressed either NELFA-WT or NELF-ΔIDR fused to GFP as indicated.
J. Western blot analysis of NELFA in HeLa cell extracts expressing tetracyclineinducible NELFA-GFP. Cells were treated with either siRNA NON or siRNA 3'UTR NELFA.
K. Fluorescence microscopy images of HeLa cells expressing mCherry fused to either NELFA-WT or NELFA-ΔIDR. NHS: No heat shock; HS: heat shock. Scale bar indicates 10 μm.
L. Percentage of cells with NELFA condensates after heat shock. Quantification of J. Cells expressed either mCherry fused NELFA-WT or NELFA-ΔIDR. Error bars represent S.D. (n = 3 independent replicates). Asterisks denote P-value <0.001 as calculated by two-tailed unpaired t-test.

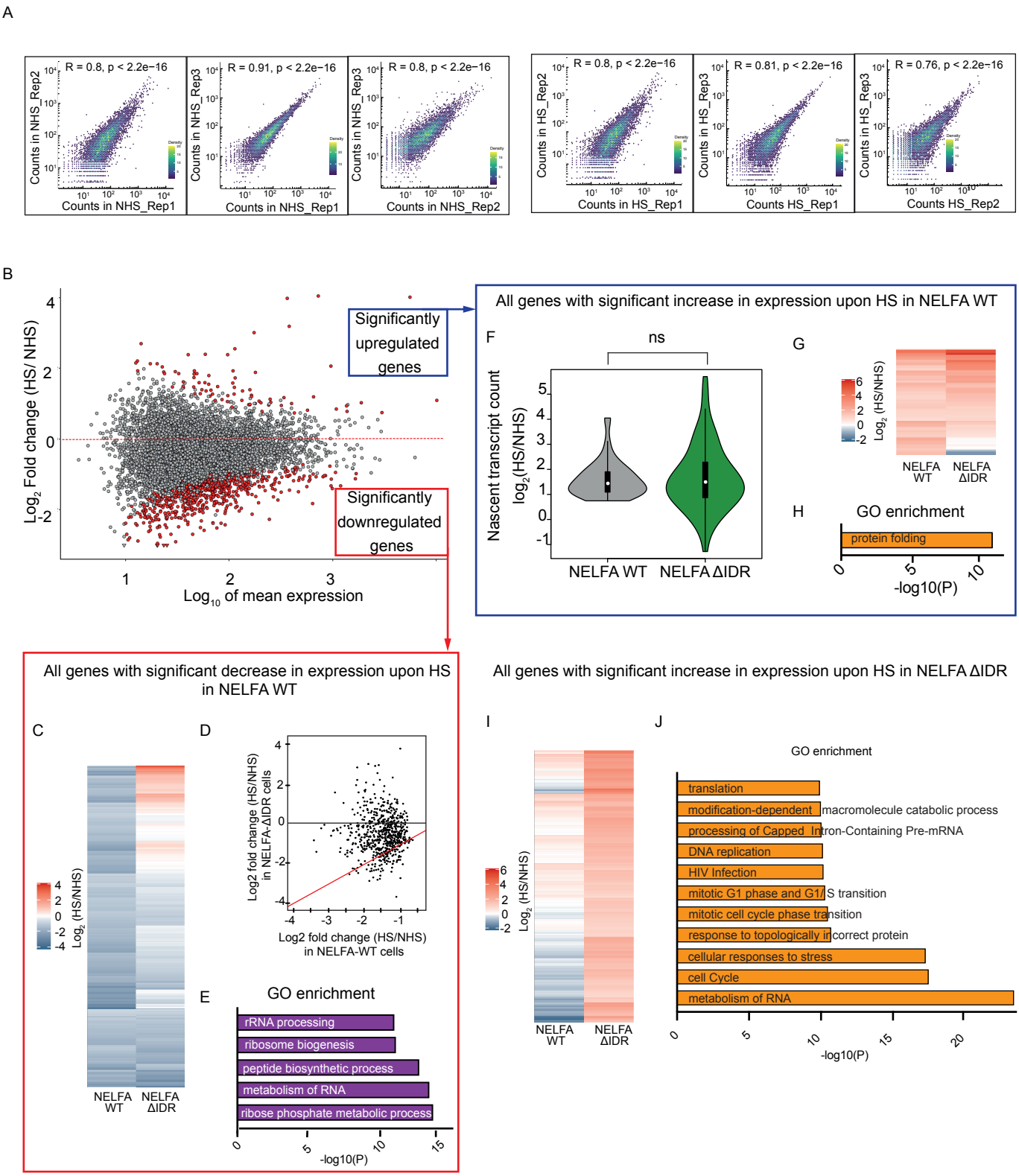


Figure S7 - NELFA-WT and NELFA-ΔIDR mutants have differential transcriptional effects
Related to Figure 6

**Figure S7. NELFA-WT and NELFA-ΔIDR cells show differential transcriptional regulation upon heat shock. Related to Figure 6.**

A. Correlation of normalized counts in 3'UTR regions from SLAM-Seq datasets (NELFA-WT) between replicates. R and p values are calculated using spearman correlation method.
B. Change in nascent transcription measured by SLAM-seq in heat-shocked (HS) compared to non-heat-shocked (NHS) HeLa cells plotted against mean expression. Genes with significant changes in nascent transcript count ($P < 0.1$ based on DESeq2-analysis, $n = 3$ independent replicates) are indicated in red. 626 genes were significantly downregulated and are further analyzed in panel C-E. 80 genes were significantly upregulated and are further analyzed in panel F-H.
C. Heat-maps showing log2 fold change in gene expression upon heat shock for NELFA-WT and NELFA-ΔIDR conditions.
D. Scatter plot showing log2 fold change in gene expression upon heat shock in NELFA-WTand NELFA-ΔIDR conditions.
E. GO analysis of significantly downregulated genes from B. Pathways enriched with -log10 (P) value of more than 10 are shown.
F. Violin plot showing log2 fold change in gene expression upon heat shock in NELFA-WT and NELFA-ΔIDR conditions.
G. Heat maps showing log2 fold change in gene expression upon heat shock in NELFA-WT and NELFA-ΔIDR conditions.
H. GO analysis of significantly up-regulated genes from B. The only pathway enriched with -log10 (P) value of more than 10 is shown.
I. Heat maps showing log2 fold change upon heat shock for significantly up-regulated genes in NELFA-ΔIDR cells and comparison with same gene set in NELFA-WT conditions.
J. GO analysis of significantly up-regulated genes in NELFA-ΔIDR cells. Pathways enriched with -log10 (P) value of more than 10 are shown.

**Supplementary-Table_S1_Primer Sequences (Related to Key Resource Table)**

| S.No. | Primer Sequence | Primer Name | Experiment used |
|---|---|---|---|
| | | | |
| 1 | GGAAGCTTCTGAGCGTGATA | RPL37_Fwd | NELFA_ChIP_Primers |
| 2 | CAGGCACCAGTTAGCAGTCA | RPL37_Rev | NELFA_ChIP_Primers |
| 3 | CTGTCGTGGCGTCTTGCTTT | RPS3A_Fwd | NELFA_ChIP_Primers |
| 4 | CTACGCCGCGATCTAGGACC | RPS3A_Rev | NELFA_ChIP_Primers |
| 5 | TCTTCCTTCTCGCCTAACGC | RPL14_Fwd | NELFA_ChIP_Primers |
| 6 | GGAGCCCGCAACAGTAAGAC | RPL14_Rev | NELFA_ChIP_Primers |
| 7 | GGAGCTCGGTGATCACATTT | NoPeak_Fwd | NELFA_ChIP_Primers |
| 8 | CGTCTAGGAGCCAACTGAGG | NoPeak_Rev | NELFA_ChIP_Primers |
| | | | |
| 9 | agctcacaccatgtcactcg | TUBB4B_Fwd | Intron-Exon Nascent transcript qPCR |
| 10 | GCTCTCAGCCTCCTTTCTCA | TUBB4B_Rev | Intron-Exon Nascent transcript qPCR |
| 11 | ttgcaattggagtagccataga | TUBA1C_Fwd | Intron-Exon Nascent transcript qPCR |
| 12 | CTCCAGCTTGGACTTCTTGC | TUBA1C_Rev | Intron-Exon Nascent transcript qPCR |
| 13 | aggccattggtctagggagt | RPS14_Fwd | Intron-Exon Nascent transcript qPCR |
| 14 | GAGTGCTGTCAGAGGGGATG | RPS14_Rev | Intron-Exon Nascent transcript qPCR |
| 15 | GTGGTTGGTGTACAGGGAGA | RPL38_Fwd | Intron-Exon Nascent transcript qPCR |
| 16 | GCCTGTTTTGGGTAATGGGG | RPL38_Rev | Intron-Exon Nascent transcript qPCR |
| 17 | CATCCCGTGTCAACAATGGT | LDHB_Fwd | Intron-Exon Nascent transcript qPCR |
| 18 | TTTCTGCCCTTGCTGTCCAA | LDHB_Rev | Intron-Exon Nascent transcript qPCR |
| 19 | TGCACCACCAACTGCTTAGC | GAPDH_Fwd | Intron-Exon Nascent transcript qPCR |
| 20 | GGCATGGACTGTGGTCATGAG | GAPDH_Rev | Intron-Exon Nascent transcript qPCR |
| 21 | GGATGACTACTTAAATGTAAAAAAGT | EEF1A1_fwd | Intron-Exon Nascent transcript qPCR |
| 22 | GAGCTTTCTGGGCAGACTTG | EEF1A1_Rev | Intron-Exon Nascent transcript qPCR |
| 23 | GTTCTCAACTTCCCAGGAGT | ENO1_Fwd | Intron-Exon Nascent transcript qPCR |
| 24 | GAGGGGTCTGTGTAGCCAAC | ENO1_Rev | Intron-Exon Nascent transcript qPCR |
| 25 | ACTGGCTGCAAAGGATTAGGAT | HNRNPA2B1_Fwd | Intron-Exon Nascent transcript qPCR |
| 26 | ATAACCCCCACTTCCTCCAC | HNRNPA2B1_Rev | Intron-Exon Nascent transcript qPCR |
| 27 | ACTTGCTGATCTCTGGGTCC | RPS19_Fwd | Intron-Exon Nascent transcript qPCR |
| 28 | GAAGCACCCAGATTTCAGCC | RPS19_Rev | Intron-Exon Nascent transcript qPCR |
| | | | |
| 29 | GGCTTCATGGCCGGCTCC | NELFA_Delta_Fwd Deletion aa 321-460 | SDM cloning |
| 30 | GGGCAGCGCAGGCTCATT | NELFA_Delta_Rev Deletion aa 321-460 | SDM cloning |
| 31 | ctcgaagcttTACCCAACTTTCTTGTACAAAG | Insertion of restriction site_Fwd_1 | IDR Replacement Cloning |
| 32 | ctttcctcgagGGACACATTGGTCATGGG | Insertion of restriction site_Rev_1 | IDR Replacement Cloning |
| 33 | agcaagcttTACCCAACTTTCTTGTACAAAG | Insertion of restriction site_Fwd_2 | IDR Replacement Cloning |
| 34 | ttcctcgagGGACACATTGGTCATGGG | Insertion of restriction site_Rev_2 | IDR Replacement Cloning |
| 35 | GGAAGCCTCGAGagccagaacacaggctat | FUS_Fwd IDR Amplification aa 61-260 | IDR Replacement Cloning |
| 36 | GCTTCCAAGCTTaccacggtcacttccgcc | FUS_Rev IDR Amplification aa 61-260 | IDR Replacement Cloning |
| 37 | GGAAGCCTCGAGcagcctgcttatccagcc | EWSR1_Fwd IDR Amplification aa 121-340 | IDR Replacement Cloning |
| 38 | GCTTCCAAGCTTatccatgggtccaccaggctt | EWSR1_Rev IDR Amplification aa 121-340 | IDR Replacement Cloning |
| | | | |
| 39 | GUAUAGUUGUGGACAUUUAUU | Duplex 1 : Length: 21 : Sense | NELFA 3'UTR siRNA #1 |
| 40 | UAAAUGUCCACAACUAUACUU | Duplex 1 : Length: 21 : Antisense | NELFA 3'UTR siRNA #1 |
| 41 | UUGUAUAGUUGUGGACAUUUU | Duplex 2 : Length: 21 : Sense | NELFA 3'UTR siRNA #2 |
| 42 | AAUGUCCACAACUAUACAAUU | Duplex 2 : Length: 21 : Antisense | NELFA 3'UTR siRNA #2 |
| 43 | UUUAAGUUCUGGAUGCAUUUU | Duplex 3 : Length: 21 : Sense | NELFA 3'UTR siRNA #3 |
| 44 | AAUGCAUCCAGAACUUAAAUU | Duplex 3 : Length: 21 : Antisense | NELFA 3'UTR siRNA #3 |